On Quartically-Solvable Robots

Nicolás Rojas, Júlia Borràs, and Federico Thomas

Abstract— **This paper presents a first attempt at a unified kinematics analysis of all serial and parallel solvable robots, that is, robots whose position analysis can be carried out without relying on numerical methods. The efforts herein are focused on finding a unified formulation for all quartically-solvable robots, as all other solvable robots can be seen as particular cases of them. The first part is centered on the quest for the most general quartically-solvable parallel and serial robots. As a result, representatives of both classes are selected. Then, using Distance Geometry, it is shown how solving the forward kinematics of the parallel representative is equivalent to solve the inverse kinematics of the serial representative, thus providing a unified formulation. Finally, it is shown that the position and singularity analysis of these robots reduces to the analysis of the relative position of two coplanar ellipses.**

I. Introduction

A serial/parallel robot is said to be *solvable* if its inverse/forward kinematics can be solved by computing the roots of polynomials up to order four. Since the Abel-Ruffini theorem states that the roots of polynomials of degree five or higher cannot be expressed, in general, in terms of additions, subtractions, multiplications, divisions, and square root extractions, a solvable robot is a robot whose position analysis can be carried out without relying on numerical methods.

Among all solvable robots, those that require the solution of quartic polynomials, or *quartically-solvable robots*, are the most general ones as all other solvable robots can be seen as particular cases of them.

In general, we can make any non-solvable robot solvable by introducing some extra geometric constraints —such as congruency, coincidence, paralelism, colinearity, coplanarity, etc.— between the geometric elements defining their joints. A plethora of quartically-solvable robots can thus be derived. Nevertheless, we are only interested in genuinely quartically-solvable robots, that is, robots that are quartically-solvable when their joints are placed arbitrarily.

While the quintessential quartically-solvable serial robot is the 3R regional robot [1], [2], at least 5 quartically-solvable parallel robots, with no apparent connection between them (see Fig.1), have been identified in the literature. Nevertheless, we next show that, using singularity-invariant transformations, these 5 robots can be seen to belong to two different classes [3].

N. Rojas is with the Department of Mechanical Engineering and Materials Science, Yale University, USA. nicolas.rojas@yale.edu

J. Borràs is with the Karlsruhe Institute of Technology, Hermann-von-Helmholtz-Platz 1, 76344 Eggenstein-Leopoldshafen, Germany. juliaborras@gmail.com

F. Thomas is with the Institut de Robòtica i Informàtica Industrial (CSIC-UPC), Llorens Artigas 4-6, 08028 Barcelona, Spain. fthomas@ri.upc.edu.

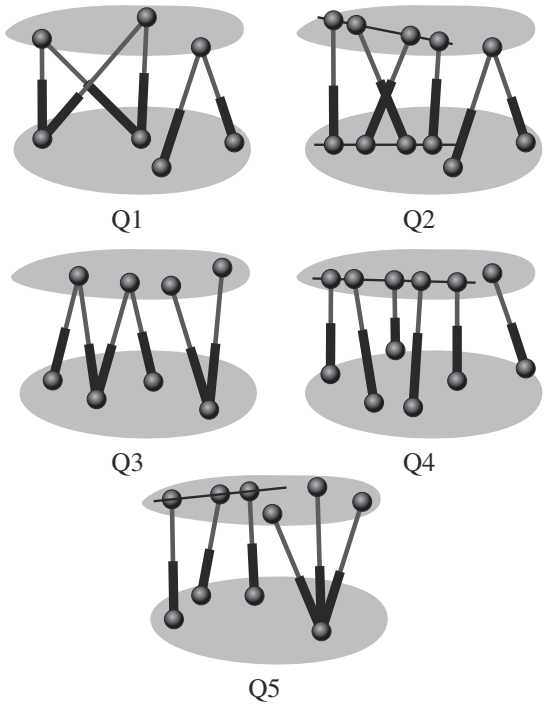

Fig. 1. Five quartically-solvable parallel robots. The joints of Q1 can be placed arbitrarily. On the contrary, Q2 requires two alignments; Q3, 1 alignment and 1 coplanarity; Q4, 2 coplanarities; and Q5, 2 coplanarities and 1 alignment. Using singularity-invariant transformations, it can be seen that they belong to two different classes. See text for details.

Two parallel robots are said to be connected through a singularity-invariant transformation if, for the same pose of their moving platforms with respect to the base, the squared leg lengths of one robot can be affinely expressed in the terms of the squared leg lengths of the other. Then, if the forward kinematics of any of the two robots is solved, the same problem is automatically solved for the other. Moreover, it is easy to prove that both robots have the same singularity locus, and hence the name of this kind of transformations. Space limitations prevents us from giving a detailed description of these transformations, but the interested reader can find a summary in [4].

Now, observe that Q1 contains a line-line and a point-line component [5]. The multiple spherical joints in the line-line component can be eliminated by using the singularity-invariant transformation presented in [6]. This leads to Q2. Thus, the kinematics analysis of both, Q1 and Q2, can be said to be equivalent.

Q3 is another parallel robot that was proved to be quartically-solvable provided that the joints in the base and

the moving platform are coplanar [7]. It was also studied in [8] were it was shown that the number of its assembly modes remains the same if the coplanarity constraints are relaxed, in which case it is not longer solvable. Since it contains a line-point component, the singularity-invariant transformation presented in [6] can be applied to rearrange the joints in the line so that a line-plane component arises. Then, the singularity-invariant transformation for line-plane components described in [6] can be applied to derive Q4, a parallel robot already studied in [9]. This uncovers an unnoticed connection between the results presented in [9] and [7]. Finally, as explained in [10], a bit more complicated sequence of transformations permits to derive Q5 from Q4.

Summing up, Q1 and Q3 can be seen as representatives of two different classes of quartically-solvable robots, but Q3 is not solvable if the coplanarity constraints are relaxed. Thus, it is reasonable to take Q1 as the genuine representative of the family of quartically-solvable parallel robots because the location of its joints is unconstrained.

Now, although at first glance Q1 seems to have little in common with a 3R serial robot, we will see how their position analyses are equivalent in spite of their disparate number of degrees of freedom, and how this equivalence have important repercussions for their singularity analysis. This paper is essentially devoted to show these facts.

This paper is organized as follows. The unified formulation, using Distance Geometry, is derived in Section II. The position and the singularity analyses of quartically-solvable robots using this formulation is presented in Section III and Section IV, respectively. Section V contains an illustrative example. Finally, some conclusions and prospects for future research are given in Section VI.

II. Unified formulation

Consider the 3R and the Q1 robots depicted in Fig. 2. We have placed in each of them 7 points, $P_1, \ldots, P_7$, which define the location of their joints. Now, observe that the resulting distance graphs, having an edge when the distance between the two corresponding points does not depend on the robots' configurations, are isomorphic to the graph shown in the center of the same figure.

According to the notation used in Fig. 2, the distances between the set of points $\{P_1, P_2, P_3, P_4, P_7\}$ or $\{P_3, P_4, P_5, P_6, P_7\}$ are not independent because they are embedded in $\mathbb{R}^3$. This dependency, using the theory of Cayley-Menger determinants, which follows from Menger's intrinsic characterization of the Euclidean metric [11], translates into the following algebraic conditions:

$$\begin{vmatrix} 0 & 1 & 1 & 1 & 1 & 1 \\ 1 & 0 & s_{1,2} & s_{1,3} & s_{1,4} & s_{1,7} \\ 1 & s_{2,1} & 0 & s_{2,3} & s_{2,4} & s_{2,7} \\ 1 & s_{3,1} & s_{3,2} & 0 & s_{3,4} & s_{3,7} \\ 1 & s_{4,1} & s_{4,2} & s_{4,3} & 0 & s_{4,7} \\ 1 & s_{7,1} & s_{7,2} & s_{7,3} & s_{7,4} & 0 \end{vmatrix} = 0 \tag{1}$$

and

$$\begin{vmatrix} 0 & 1 & 1 & 1 & 1 & 1 \\ 1 & 0 & s_{3,4} & s_{3,5} & s_{3,6} & s_{3,7} \\ 1 & s_{4,3} & 0 & s_{4,5} & s_{4,6} & s_{4,7} \\ 1 & s_{5,3} & s_{5,4} & 0 & s_{5,6} & s_{5,7} \\ 1 & s_{6,3} & s_{6,4} & s_{6,5} & 0 & s_{6,7} \\ 1 & s_{7,3} & s_{7,4} & s_{7,5} & s_{7,6} & 0 \end{vmatrix} = 0, \tag{2}$$

where $s_{i,j}$ stands for the squared distance between P_i and P_j. The above two equations are quadratic forms in the unknown distances $s_{3,7}$ and $s_{4,7}$. They actually represent two real ellipses, $\mathcal{A} : \mathbf{x}\mathbf{A}\mathbf{x}^T = 0$ and $\mathcal{B} : \mathbf{x}\mathbf{B}\mathbf{x}^T = 0$, where $\mathbf{x} = (s_{3,7}, s_{4,7}, 1)$ and

$$\mathbf{A} = \begin{pmatrix} a_1 & c_1 & d_1 \\ c_1 & b_1 & e_1 \\ d_1 & e_1 & f_1 \end{pmatrix} \quad \text{and} \quad \mathbf{B} = \begin{pmatrix} a_2 & c_2 & d_2 \\ c_2 & b_2 & e_2 \\ d_2 & e_2 & f_2 \end{pmatrix}. \tag{3}$$

The entries of $\mathbf{A}$ and $\mathbf{B}$ can, in turn, be expressed in terms of determinants (see Table I).

Now, if we eliminate, for example, $s_{3,7}$ from the system formed by equations (1) and (2), a quartic closure polynomial in $s_{4,7}$ is obtained. The result cannot be included here for space limitation reasons, but it can be easily reproduce using a computer algebra system. Nevertheless, instead of using this closure quartic polynomial, we will see that it is highly advantageous to proceed using the equations of both ellipses. After all, the geometric interpretation of the solution of the general quartic polynomial reduces to the intersection of two ellipses [12].

III. Position analysis

If we have $n > 4$ points in $\mathbb{R}^3$ and we know all the pairwise distances between them, we can assign a unique set of coordinates to them up to isometries (translations, rotations and reflections). If, besides these pairwise distances, we already know the coordinates of three of these points, the coordinates are unique up to a reflection about the plane defined by these three points. If, instead of the coordinates of three points, we know the coordinates of four points, the coordinates of all other points are univocally determined. Alternatively, if we know the coordinates of three points and the orientation of a tetrahedron defined by a set of four points, the coordinates of all points are also univocally determined. From the practical point of view, these coordinates can be obtained by generate-and-test sequences of trilaterations [13].

Once we have values for $s_{3,7}$ and $s_{4,7}$ resulting from intersecting $\mathcal{A}$ and $\mathcal{B}$, then all the pairwise distances between the points in the sets $\{P_7, P_1, P_2, P_3, P_4\}$ and $\{P_7, P_3, P_4, P_5, P_6\}$ are known. In this context, the inverse kinematics of the serial 3R robot in Fig. 2 can be restated as to find the feasible location of the segments $\overline{P_3P_4}$ and $\overline{P_5P_6}$ in $\mathbb{R}^3$ given the locations of P_1, P_2, and P_7 and the orientations of the tetrahedra defined by the sets of points $\{P_1, P_2, P_3, P_4\}$ and $\{P_3, P_4, P_5, P_6\}$. The solution to this problem can be obtained in two steps:

1) Assign coordinates to P_3 and P_4. This assignment is unique because the coordinates of P_1, P_2 and

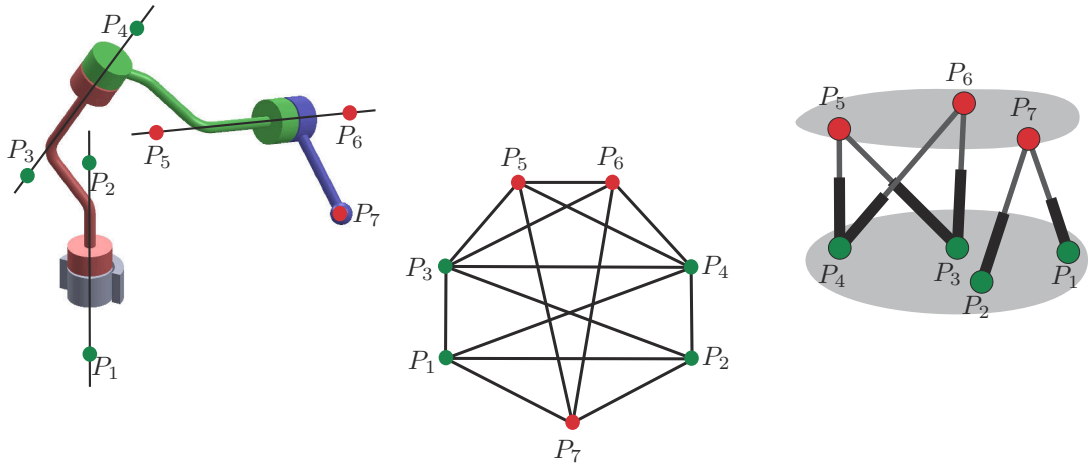

Fig. 2. The graph in the center is isomorphic to the distance graphs associated with the seven points defining the location of the joints of 3R serial robot on the left, and the parallel robot on the right.

TABLE I

COEFFICIENTS OF THE ELLIPSES $\mathcal{A}$ AND $\mathcal{B}$ EXPRESSED AS DETERMINANTS OF SQUARED DISTANCES BETWEEN $P_1, \ldots, P_7$

$$a_1 = -\begin{vmatrix} 0 & 1 & 1 & 1 \\ 1 & 0 & s_{1,2} & s_{1,4} \\ 1 & s_{1,2} & 0 & s_{2,4} \\ 1 & s_{1,4} & s_{2,4} & 0 \end{vmatrix}, \quad b_1 = -\begin{vmatrix} 0 & 1 & 1 & 1 \\ 1 & 0 & s_{1,2} & s_{1,3} \\ 1 & s_{1,2} & 0 & s_{2,3} \\ 1 & s_{1,3} & s_{2,3} & 0 \end{vmatrix}, \quad c_1 = \begin{vmatrix} 0 & 1 & 1 & 1 \\ 1 & 0 & s_{1,2} & s_{1,3} \\ 1 & s_{1,2} & 0 & s_{2,3} \\ 1 & s_{1,4} & s_{2,4} & s_{3,4} \end{vmatrix},$$

$$d_1 = -\begin{vmatrix} 0 & 1 & 1 & 1 & 1 \\ 1 & 0 & s_{1,2} & s_{1,4} & s_{1,7} \\ 1 & s_{1,2} & 0 & s_{2,4} & s_{2,7} \\ 1 & s_{1,4} & s_{2,4} & 0 & 0 \\ 1 & s_{1,3} & s_{2,3} & s_{3,4} & 0 \end{vmatrix}, \quad e_1 = -\begin{vmatrix} 0 & 1 & 1 & 1 & 1 \\ 1 & 0 & s_{1,2} & s_{1,3} & s_{1,7} \\ 1 & s_{1,2} & 0 & s_{2,3} & s_{2,7} \\ 1 & s_{1,3} & s_{2,3} & 0 & 0 \\ 1 & s_{1,4} & s_{2,4} & s_{3,4} & 0 \end{vmatrix}, \quad f_1 = \begin{vmatrix} 0 & 1 & 1 & 1 & 1 & 1 \\ 1 & 0 & s_{1,2} & s_{1,3} & s_{1,4} & s_{1,7} \\ 1 & s_{1,2} & 0 & s_{2,3} & s_{2,4} & s_{2,7} \\ 1 & s_{1,3} & s_{2,3} & 0 & s_{2,4} & 0 \\ 1 & s_{1,4} & s_{2,4} & s_{3,4} & 0 & 0 \\ 1 & s_{1,7} & s_{2,7} & 0 & 0 & 0 \end{vmatrix},$$

$$a_2 = -\begin{vmatrix} 0 & 1 & 1 & 1 \\ 1 & 0 & s_{5,6} & s_{5,4} \\ 1 & s_{5,6} & 0 & s_{6,4} \\ 1 & s_{5,4} & s_{6,4} & 0 \end{vmatrix}, \quad b_2 = -\begin{vmatrix} 0 & 1 & 1 & 1 \\ 1 & 0 & s_{5,6} & s_{5,3} \\ 1 & s_{5,6} & 0 & s_{6,3} \\ 1 & s_{5,3} & s_{6,3} & 0 \end{vmatrix}, \quad c_2 = \begin{vmatrix} 0 & 1 & 1 & 1 \\ 1 & 0 & s_{5,6} & s_{5,3} \\ 1 & s_{5,6} & 0 & s_{6,3} \\ 1 & s_{5,4} & s_{6,4} & s_{3,4} \end{vmatrix},$$

$$d_2 = -\begin{vmatrix} 0 & 1 & 1 & 1 & 1 \\ 1 & 0 & s_{5,6} & s_{5,4} & s_{5,7} \\ 1 & s_{5,6} & 0 & s_{2,4} & s_{6,7} \\ 1 & s_{5,4} & s_{6,4} & 0 & 0 \\ 1 & s_{5,3} & s_{6,3} & s_{3,4} & 0 \end{vmatrix}, \quad e_2 = -\begin{vmatrix} 0 & 1 & 1 & 1 & 1 \\ 1 & 0 & s_{5,6} & s_{5,3} & s_{5,7} \\ 1 & s_{5,6} & 0 & s_{6,3} & s_{6,7} \\ 1 & s_{5,3} & s_{6,3} & 0 & 0 \\ 1 & s_{5,4} & s_{6,4} & s_{3,4} & 0 \end{vmatrix}, \quad f_2 = \begin{vmatrix} 0 & 1 & 1 & 1 & 1 & 1 \\ 1 & 0 & s_{5,6} & s_{5,3} & s_{5,4} & s_{5,7} \\ 1 & s_{5,6} & 0 & s_{6,3} & s_{6,4} & s_{6,7} \\ 1 & s_{5,3} & s_{6,3} & 0 & s_{3,4} & 0 \\ 1 & s_{5,4} & s_{6,4} & s_{3,4} & 0 & 0 \\ 1 & s_{5,7} & s_{6,7} & 0 & 0 & 0 \end{vmatrix}.$$

P_7 are known and the orientation of the tetrahedron $\{P_1, P_2, P_3, P_4\}$ is fixed.

2) Assign coordinates to P_5 and P_6. Again, the assignment is unique because the coordinates of P_3, P_4 and P_7 are known and the orientation of the tetrahedron $\{P_3, P_4, P_5, P_6\}$ is fixed.

The forward kinematics of the Q1 parallel robot in Fig. 2 can be restated as to find the feasible locations of P_5, P_6 and P_7 given the locations of P_1, P_2, P_3 and P_4. The solution can be obtained as follows:

1) Assign coordinates to P_7. This assignment is unique because the coordinates of P_1, P_2, P_3, and P_4 are known.
2) Assign coordinates to P_5 and P_6. In this case, we have two possible assignments, one being the mirror projection of the other with respect to the plane defined by P_2, P_4, and P_7. Once the coordinates for P_6 are assigned, we have two possible assignments for those of P_5, and conversely. Both assignments would coincide if P_3, P_4, P_5, and P_6 on a plane.

As a consequence, for each intersection of $\mathcal{A}$ and $\mathcal{B}$, there is a single configuration for the 3R robot and two possible configurations for Q1. In other words, we can have up to 4 inverse kinematics solutions for a serial 3R robot and 8 forward kinematics solutions for a Q1 parallel robot. This difference between both robots is important when analyzing their singularities, but this is better explained through an example, as it is done in Section V.

IV. SINGULARITY ANALYSIS

A singularity occurs when we have a repeated solution of the inverse/forward kinematics, that is, when $\mathcal{A}$ and $\mathcal{B}$ are tangent. The positional relationship between $\mathcal{A}$ and $\mathcal{B}$ can be derived from the study of the pencil of conics they define, that is, from the family of conics defined by $\mathbf{p}^T(\lambda\mathbf{A}+\mathbf{B})\mathbf{p} = 0$, $\lambda \in \mathbb{R}$ (see [14] for an introductory explanation). The

values of λ for which a conic of this pencil is degenerate correspond to those in which

$$f(\lambda) = \det(\lambda\mathbf{A} + \mathbf{B}) = l_3\lambda^3 + 3l_2\lambda^2 + 3l_1\lambda + l_0 = 0, \quad (4)$$

where the coefficients l_i, $i = 0, 1, 2, 3$, can expressed in a neat and elegant way as [15, p. 191]:

$$l_3 = \begin{vmatrix} a_1 & c_1 & d_1 \\ c_1 & b_1 & e_1 \\ d_1 & e_1 & f_1 \end{vmatrix} = \det(\mathbf{A}), \quad (5)$$

$$3l_2 = \begin{vmatrix} a_2 & c_1 & d_1 \\ c_2 & b_1 & e_1 \\ d_2 & e_1 & f_1 \end{vmatrix} + \begin{vmatrix} a_1 & c_2 & d_1 \\ c_1 & b_2 & e_1 \\ d_1 & e_2 & f_1 \end{vmatrix} + \begin{vmatrix} a_1 & c_1 & d_2 \\ c_1 & b_1 & e_2 \\ d_1 & e_1 & f_2 \end{vmatrix}, \quad (6)$$

$$3l_1 = \begin{vmatrix} a_1 & c_2 & d_2 \\ c_1 & b_2 & e_2 \\ d_1 & e_2 & f_2 \end{vmatrix} + \begin{vmatrix} a_2 & c_1 & d_2 \\ c_2 & b_1 & e_2 \\ d_2 & e_1 & f_2 \end{vmatrix} + \begin{vmatrix} a_2 & c_2 & d_1 \\ c_2 & b_2 & e_1 \\ d_2 & e_2 & f_1 \end{vmatrix}, \quad (7)$$

$$l_0 = \begin{vmatrix} a_2 & c_2 & d_2 \\ c_2 & b_2 & e_2 \\ d_2 & e_2 & f_2 \end{vmatrix} = \det(\mathbf{B}). \quad (8)$$

The above polynomial in λ is known as the *generalized characteristic polynomial* of the pencil.

When the two ellipses defining the pencil are tangent, two of the three degenerate conics in the pencil become identical. This implies that the characteristic equation of the pencil has a repeated root for λ [16]. By definition, $f(\lambda) = 0$ has a multiple root if, and only if, its discriminant, say Δ, vanishes. Furthermore, it can be shown that $f(\lambda) = 0$ has three simple real roots if $\Delta > 0$, and $f(\lambda) = 0$ has two complex conjugate roots and a real root if $\Delta < 0$. Then, the roots of $\Delta = 0$ give information on the positional relationship between $\mathcal{A}$ and $\mathcal{B}$. Actually, the sign of the discriminant Δ gives information about the order of accessibility of the robot's workspace. It permits to decompose it in the following three regions:

- $\Delta < 0$ corresponds to a two-way (four-way) accessible region of the 3R robot (Q1 robot);
- $\Delta = 0$ corresponds to singularities of the robot; and
- $\Delta > 0$ corresponds to a four-way (eight-way) accessible region or an inaccessible region of the 3R robot (Q1 robot).

The discriminant of a cubic conveniently expressed as follows [17]:

$$\Delta = \begin{vmatrix} 2\delta_1 & \delta_2 \\ \delta_2 & 2\delta_3 \end{vmatrix} \quad (9)$$

where

$$\delta_1 = \begin{vmatrix} l_3 & l_2 \\ l_2 & l_1 \end{vmatrix}, \quad \delta_2 = \begin{vmatrix} l_3 & l_1 \\ l_2 & l_0 \end{vmatrix}, \quad \text{and} \quad \delta_3 = \begin{vmatrix} l_2 & l_1 \\ l_1 & l_0 \end{vmatrix}. \quad (10)$$

Observe that the condition of singularity $\Delta = 0$ is expressed as a determinant of determinants of determinants of determinants (four levels of nested determinants). It can be shown that the elements of the third level of determinants depend quadratically on $s_{3,7}$ and $s_{4,7}$. Then, since the two outer levels of determinants are quadratic with respect to their elements, the singularity locus can be displayed as a curve of order 2^3 in the plane defined by $s_{1,7}$ and $s_{2,7}$.

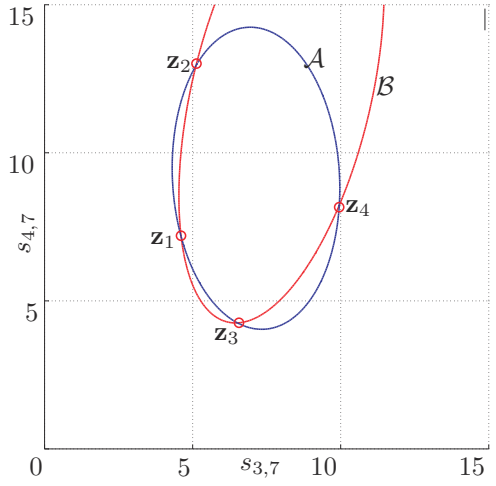

Fig. 3. The ellipses $\mathcal{A}$ and $\mathcal{B}$ for the serial and parallel quartically-solvable robots analyzed as an example.

V. Example

Let us consider a serial and a parallel robot with the same topologies as the ones depicted in Fig. 2 with

$$\mathbf{S} = \begin{pmatrix} 0 & 4 & 2 & 6 & ? & ? & 4 \\ 4 & 0 & 2 & 6 & ? & ? & 12 \\ 2 & 2 & 0 & 4 & 0.89 & 4.89 & ? \\ 6 & 6 & 4 & 0 & 2.89 & 6.89 & ? \\ ? & ? & 0.89 & 2.89 & 0 & 4 & 6.25 \\ ? & ? & 4.89 & 6.89 & 4 & 0 & 2.25 \\ 4 & 12 & ? & ? & 6.25 & 2.25 & 0 \end{pmatrix}, \quad (11)$$

where $s_{i,j} = \mathbf{S}(i, j)$. Then, substituting these squared distances in (1) and (2), we obtain

$$\mathcal{A} : \begin{pmatrix} s_{3,7} & s_{4,7} \end{pmatrix} \begin{pmatrix} 80 & -16 & -448 \\ -16 & 16 & -64 \\ -448 & -64 & 3584 \end{pmatrix} \begin{pmatrix} s_{3,7} \\ s_{4,7} \end{pmatrix} = 0, \quad (12)$$

and

$$\mathcal{B} : \begin{pmatrix} s_{3,7} & s_{4,7} \end{pmatrix} \begin{pmatrix} 46.2 & 1.8 & -346.2 \\ 1.8 & 14.2 & -142.7 \\ -346.2 & -142.7 & 340.8 \end{pmatrix} \begin{pmatrix} s_{3,7} \\ s_{4,7} \end{pmatrix} = 0, \quad (13)$$

whose intersection points are (see Fig. 3):

$$\mathbf{z}_1 = (4.613, 7.162), \quad \mathbf{z}_3 = (6.514, 4.256),$$
$$\mathbf{z}_2 = (5.113, 12.940), \quad \mathbf{z}_4 = (9.953, 8.231).$$

Using the procedures given in Section III, it is possible to obtain the 4 inverse kinematics solutions and the 8 assembly modes of the studied serial and parallel robot, respectively. Fig. 4 shows the inverse kinematics solutions for the serial robot in the case in which $\mathbf{p}_1 = (0, 0, 0)^T$, $\mathbf{p}_2 = (0, 0, 2)^T$, and $\mathbf{p}_7 = (1.414, 1, -1)^T$. Fig. 5 shows the resulting assembly modes for the parallel robot in the case in which $\mathbf{p}_1 = (0, 0, 0)^T$, $\mathbf{p}_2 = (0, 0, 2)^T$, $\mathbf{p}_3 = (0.919, 0.394, 1)^T$, and $\mathbf{p}_4 = (0.132, 2.232, 1)^T$.

To analyze the singularities of the serial robot, we have to treat $s_{1,7}$ and $s_{2,7}$ as variables. In this case, (9) defines

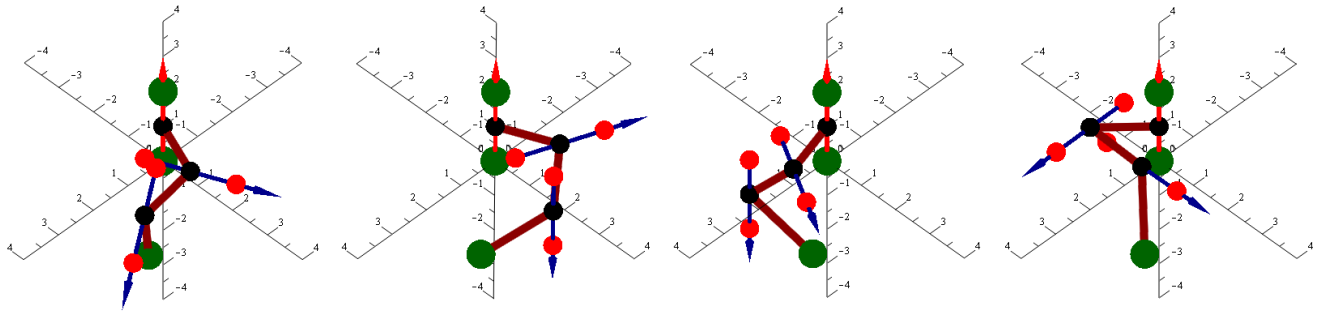

Fig. 4. The four inverse kinematics solutions for the analyzed 3R serial robot with $\mathbf{p}_1 = (0,0,0)^T$, $\mathbf{p}_2 = (0,0,2)^T$, and $\mathbf{p}_7 = (1.414,1,-1)^T$ depicted in green.

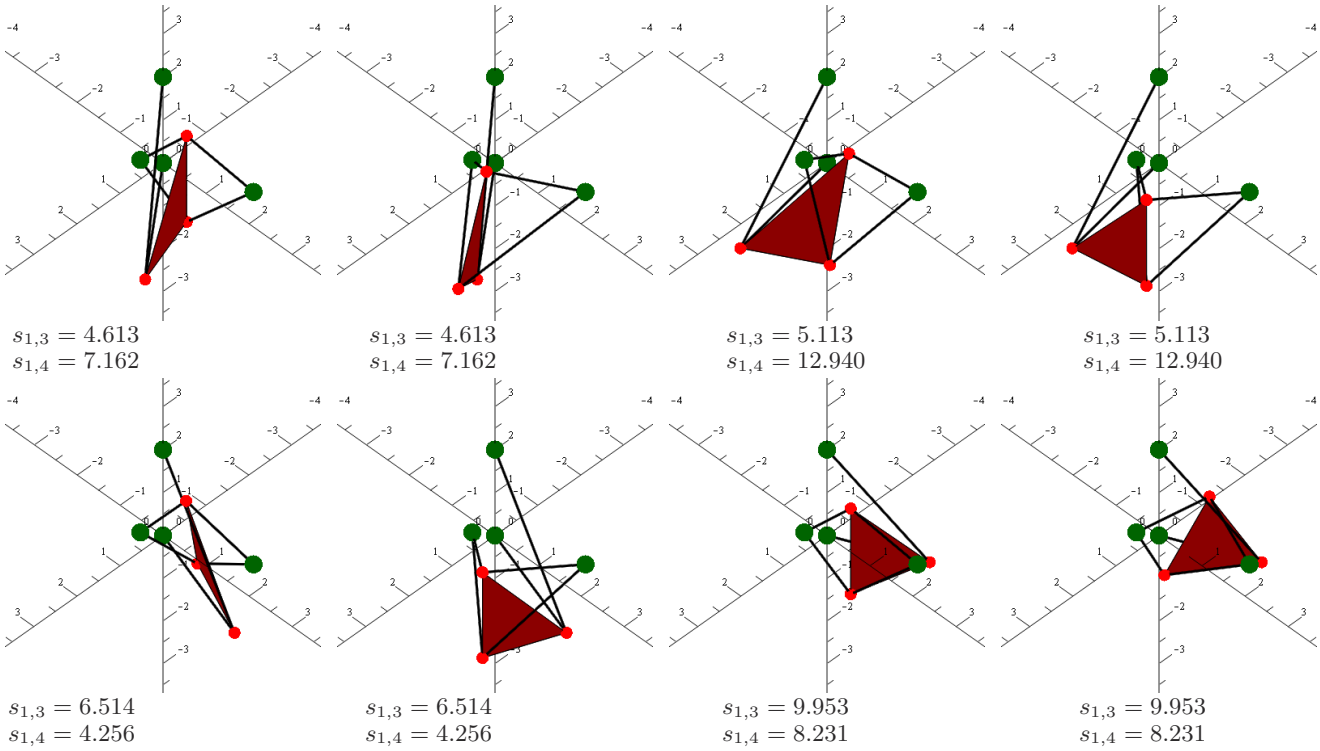

Fig. 5. The eight forward kinematics solutions for the analyzed parallel robot with $\mathbf{p}_1 = (0,0,0)^T$, $\mathbf{p}_2 = (0,0,2)^T$, $\mathbf{p}_3 = (0.919,0.394,1)^T$, and $\mathbf{p}_4 = (0.132,2.232,1)^T$ depicted in green.

a curve in the plane defined by $(s_{1,7}, s_{2,7})$. This curve is plotted in Fig. 6(left). It segments the plane into regions with the same number of intersections between $\mathcal{A}$ and $\mathcal{B}$. This singularity locus, defined in the space of squared distances, can be straightforwardly mapped onto the robot's workspace. Indeed, if we represent the location of the end-effector of the 3R robot using cylindrical coordinates given by (ρ, θ, z), then

$$z = \frac{s_{1,2} - s_{2,7} + s_{1,7}}{2\sqrt{s_{1,2}}}, \quad \rho = +\sqrt{s_{2,7} - (d_{1,2} - z)^2}. \quad (14)$$

This mapping is independent of θ because the singularity locus has a a symmetry respect to the axis defined by P_1 and P_2 (in this case, the z-azis). The result is plotted in Fig. 6(right).

In the case of the parallel robot singularities, we have to treat $s_{1,7}$, $s_{2,7}$, $s_{3,5}$, $s_{3,6}$, $s_{4,5}$, and $s_{4,6}$ as variables. Four slices of this singularity locus are plotted in Fig. 7. At this point we have also to take into account that, in this case, each intersection of $\mathcal{A}$ and $\mathcal{B}$ does not lead to a single configuration for the robot, but two. This introduces an extra singularity that corresponds to the case in which P_3, P_4, P_5, and P_6 are coplanar, as described in Section III. That is, when

$$\begin{vmatrix} 0 & 1 & 1 & 1 & 1 \\ 1 & 0 & s_{3,4} & s_{3,5} & s_{3,6} \\ 1 & s_{3,4} & 0 & s_{4,5} & s_{4,6} \\ 1 & s_{3,5} & s_{4,5} & 0 & s_{5,6} \\ 1 & s_{3,6} & s_{4,6} & s_{5,6} & 0 \end{vmatrix} = 0, \quad (15)$$

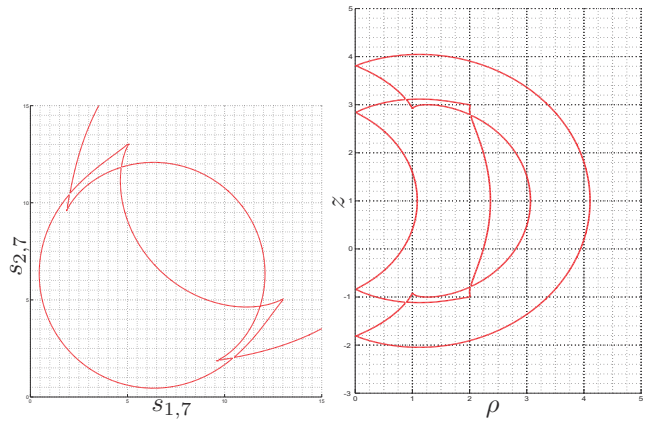

Fig. 6. Singularity locus of the analyzed 3R robot in the space of squared distances (left), and the same plot mapped onto the robot's workspace (right).

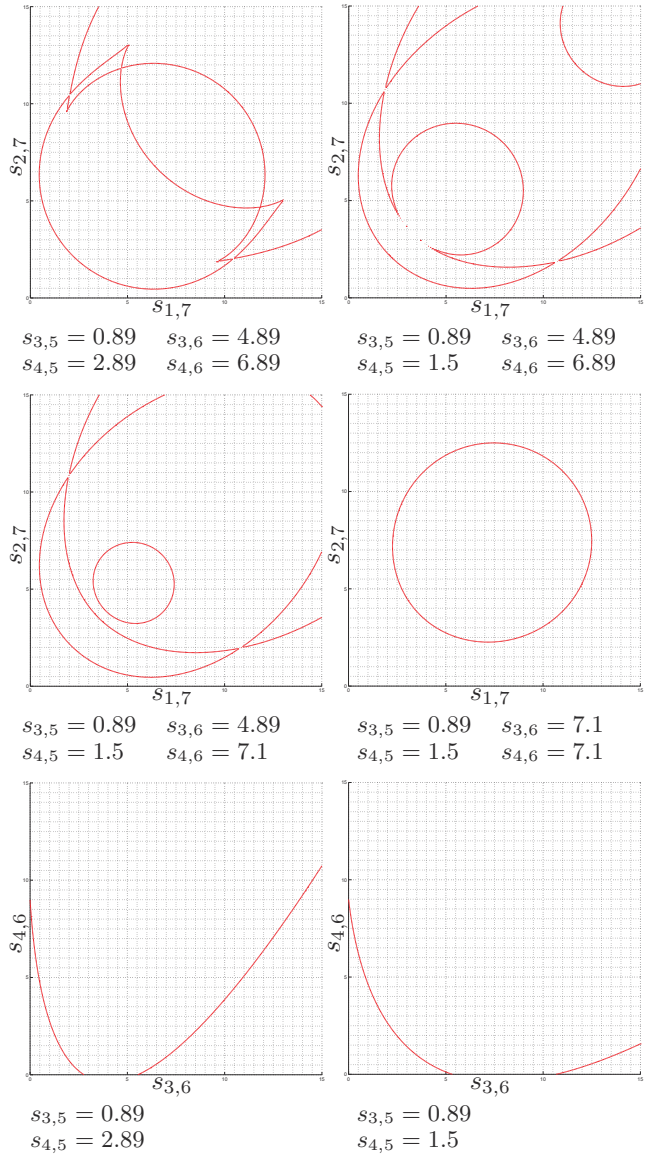

Fig. 7. Six slices of the singularity locus of the analyzed parallel robot in its operational space. Observe how one of these slices is identical to the singularity locus of the analyzed 3R robot.

which is independent of $s_{1,7}$ and $s_{2,7}$. Two slices of this singularity, for fixed values of $s_{3,5}$ and $s_{4,5}$, are also plotted in Fig. 7.

VI. Conclusion

A unified formulation for the position and singularity analysis of quartically-solvable robots has been presented, which boils down to study the positional relationship between two coplanar ellipses. This formulation paves thus the way for the development of a general theory of solvable robots. As a first step, it should be verified that all quadratically-solvable robots correspond to those cases in which at least one of these two ellipses degenerate into two lines.

Finally, it is worth observing that the singularity loci of quartically-solvable robots contain, in general, cusps, which suggests the possibility of changing the assembly/working modes of these robots without meeting a singularity. This has extensively been studied for 3R robots, but now, thanks to the unified formulation presented in this paper, the strategies for working mode changing developed for this kind of robots can directly applied to the Q1 parallel robot and all other parallel robot that can be deduced from it using singularity-invariant transformations.

References

[1] D.L. Pieper, *The kinematics of manipulators under computer control*, PhD Dissertation, Stanford University, 1968.

[2] D.R. Smith, *Design of solvable 6R manipulators*, PhD Dissertation, Georgia Institute of Technology, 1990.

[3] J. Borràs, *Singularity-Invariant Leg Rearrangements in Stewart-Gough Platforms*, PhD Dissertation, Technical University of Catalonia, 2011.

[4] J. Borràs, F. Thomas, and C. Torras, "New geometric approaches to the analysis and design of Stewart-Gough platforms," *IEEE/ASME Trans. on Mechatronics*, vol. 19, no. 2, pp. 445-455, 2014.

[5] X. Kong and C.M. Gosselin, "Classification of 6-SPS parallel manipulators according to their components," *Proceedings of 2000 ASME Design Technical Conferences*, DETC2000/MECH-14105, 2000.

[6] J. Borràs, F. Thomas, and C. Torras, "On Delta transforms," *IEEE Trans. on Robotics*, vol. 25, no. 6, pp. 1225-1236, 2009.

[7] W. Lin, M. Griffis, and J. Duffy, "Forward displacement analyses of the 4-4 Stewart platforms," *Journal of Mechanical Design*, vol. 114, no. 3, pp. 444-450, 1992.

[8] K.H. Hunt and E.J.F. Primrose, "Assembly configurations of some in-parallel-actuated manipulators," *Mechanism and Machine Theory*, vol. 28, no. 1, pp. 31-42, 1993.

[9] C. Zhang and S.M. Song, "Forward kinematics of a class of parallel (Stewart) platforms with closed-form solutions," *Journal of Robotic Systems,* vol. 9, no. 1, pp. 93-112, 1992.

[10] J. Borràs, F. Thomas, and C. Torras, "Singularity-invariant families of a class of 5-SPU platforms," *IEEE Trans. on Robotics*, vol. 27, no. 5, pp. 837-848, 2011.

[11] L. Blumenthal, *Theory and Applications of Distance Geometry*, Clarendon Press, Oxford, 1953.

[12] W.M. Faucette, "A geometric interpretation of the solution of the general quartic polynomial," *The American Mathematical Monthly*, Vol. 103, No. 1, pp. 51-57, 1996.

[13] N. Rojas, *Distance-Based Formulations for the Position Analysis of Kinematic Chains*, PhD Dissertation, Technical University of Catalonia, 2012.

[14] Y-K. Choi, W. Wang, Y. Liu, and M-S. Kim, "Continuous collision detection for two moving elliptic disks," *IEEE Trans. on Robotics,* Vol. 22, No. 2, pp. 213-224, 2006.

[15] J. Richter-Gebert, *Perspectives on Projective Geometry: A Guided Tour Through Real and Complex Geometry*, Springer, 2011.

[16] G. Salmon, *A Treatise on Conic Sections*, Chelsea Publishing Co., 1869.

[17] J.F. Blinn, Polynomial discriminants I. Matrix magic, *IEEE Computer Graphics and Applications*, Vol. 20, No. 6, pp. 94-98, 2002.